

Electron–optical-phonon scattering rates in spherical CdSe quantum dots in an external magnetic field

A. M. Alcalde and G. E. Marques

Departamento de Física, Universidade Federal de São Carlos, Caixa Postal 676, 13565-905 São Carlos SP, Brazil

(Received 31 May 2001; revised manuscript received 4 October 2001; published 12 February 2002)

We calculate electron-phonon relaxation rates in CdSe spherical quantum dots in the presence of the quantizing magnetic field. The calculated scattering rates include the contributions of the confined and surface optical modes as obtained from the dielectric continuum model. The electron states are calculated within the strong-perturbation approximation. The effects of the competing contributions of the magnetic and spatial confinement on the optical-phonon scattering rates are studied. The enhancement of the scattering rates in the strong magnetic fields regime and the possibility of tuning efficient scattering channels are also discussed.

DOI: 10.1103/PhysRevB.65.113301

PACS number(s): 73.21.–b, 63.20.Kr, 71.38.–k

The interaction between electrons and phonons is an important ingredient for any realistic discussion of the optical properties of quantum dots.^{1–4} It has considerable relevance in determining the fast carrier dynamics at small semiconductor devices and in the study of radiative transitions for photonic devices. In semiconductor quantum dots not only the electronic levels but also the lattice vibrational modes become fully discrete due to the three-dimensional confinement. It has been found that the LO-phonon spectrum in a spherical quantum dot consists of confined and surface modes, the latter being directly associated with the interfaces. Klein *et al.*,⁵ based on a dielectric continuum approach, have derived expressions for the eigenfunctions corresponding to the confined and surface phonon modes and have obtained the electron-phonon coupling Hamiltonian for these modes. Additionally, a phenomenological treatment that includes the coupling between mechanical phonon displacement and electrostatic potential has also been reported.⁶ In this work, for reasons of simplicity, we will describe the phonon modes within the dielectric continuum model.

The magnetic effects in quantum dots have been studied both experimentally^{7–10} and theoretically.^{11–13} Interesting results were obtained in several optical properties like exciton fine structure, Zeeman splitting, and Landau level formation. While for the quantum wells and wires the effect of a magnetic field on the electron-phonon interaction has been studied in great detail, the discussion of the same effects on spherical quantum dots is just starting. We report the electron-phonon scattering rate calculation in spherical quantum dots under an applied magnetic field.

The presence of an axial magnetic field produces mainly two effects: (i) the magnetic field generates additional quantization rules which modify the optic properties of the nanostructures, (ii) the external magnetic field modifies the spatial symmetry of the wave functions and, in consequence, induces important variations to the electronic overlap. As a direct consequence, this induced cylindrical symmetry, superimposed to the spatial spherical symmetry of the dots, introduces emission of new phonon modes in the electron-phonon scattering, and the modifications in the scattering rates are related to the deformation of the wave functions in this new mixed symmetry. The change in the quantization, as produced by the magnetic field, allows the appearance of

new scattering channels and opens the possibility of adjusting optical properties by appropriate choices of the values for the field. The aim of the present work is to study the electron-phonon scattering rates in spherical quantum dots in the presence of a magnetic field in the z direction.

In order to calculate the electron wave functions and energy spectrum, we explore the ideas in the strong-perturbation approach proposed by Jiang¹⁵ and successfully used in the calculation of the magnetic effects on exciton and impurity binding energies^{13,16} in spherical quantum dots. This method permits us to solve problems that involve more than one potential profile in the Hamiltonian and where the *perturbation* can be comparable to the unperturbed Hamiltonian. The calculation scheme is based on the transformation of Hamiltonian system H by choosing a wave function in the form $\psi = \phi \exp(-g)$, where ϕ is the exact solution of unperturbed contribution and g is a function that can be found by a minimization procedure. After the transformation, the new Hamiltonian can be treated by the usual perturbation theory.

The Hamiltonian for an electron in a spherical quantum dot of radius R and in the presence of an external magnetic field parallel to the z direction can be written as

$$H = -\frac{\hbar^2}{2m^*} \nabla^2 + \frac{\omega_B}{2} L_z + \frac{1}{8} m^* \omega_B^2 r^2 \sin^2 \theta + V(r), \quad (1)$$

where $\omega_B = (eB/m^*c)$ is the cyclotron frequency, L_z is the z component of the angular momentum operator, and V is the potential of confinement. We consider the term $V' = \frac{1}{8} m^* \omega_B^2 r^2 \sin^2 \theta$ as the perturbation if compared with the exactly soluble problem

$$H_0 = -\frac{\hbar^2}{2m^*} \nabla^2 + \frac{\omega_B}{2} L_z + V(r). \quad (2)$$

The analytical eigenfunctions of H_0 are given by

$$\phi_{L,M} = A_L j_L(kr) Y_L^M(\theta, \phi), \quad (3)$$

where Y_L^M are the spherical harmonics, L and M are the values of the orbital momentum and its projection, respectively. $j_L(x)$ are the spherical Bessel function and A_L is its normal-

ization constant for the dot. The energy spectrum corresponding to unperturbed Hamiltonian H_0 is given by

$$E^{(0)} = \frac{\hbar^2}{2m^*} k_{nL}^2 + \frac{M}{2} \hbar \omega_B, \quad (4)$$

where we have considered a parabolic energy dispersion and our discussion will assume the infinite confinement situation where the carrier envelope function vanishes at the surface of dot, therefore each wave vector k_{nL} is obtained from the condition $j_L(k_{nL}R) = 0$. Since we are considering II-VI quantum dots embedded in an amorphous glass matrix, the assumption of infinitely high barriers is a well justified approximation. For the dot sizes and the excited energy levels considered in this work, the effects of finite barrier can be negligible.¹⁷ More marked effects in the eigenstates would appear for sizes smaller than 30 Å. In the case of dots in glass matrix, an additional factor that limits the theoretical treatment of the finite barrier is the impossibility to define an exact value for the effective mass in the glass material.

Using the idea proposed in the strong-perturbation theory, we obtain the first-order correction to the unperturbed energy as

$$E^{(1)} \propto \int e^{-2g} (\phi_{L,M}^* \nabla g \cdot \nabla \phi_{L,M}) d\mathbf{r}. \quad (5)$$

It is important to note that Eq. (1) has a nonseparable character due to the impossibility of writing the full potential V' in terms of a single coordinate or as the sum of independent coordinates. The presence of the magnetic field breaks the spherical symmetry of the initial problem by introducing a cylindrical shape to the potential that will compete with the spherical confinement potential as the value of the cyclotron radius becomes comparable to R . Some approaches have been used to describe this problem: Kim *et al.*¹⁸ obtained an analytic expression for the electronic spectrum considering that the electron only moves on the surface of the spherical potential. Nomura *et al.*¹² applied full diagonalization and calculated the exciton and absorption spectrum. This numerical method, although efficient, demands a great computational effort. Some fast-convergence numerical methods like the boundary-element method¹⁹ could also be used to solve this problem numerically. The strong-perturbation procedure used in this work allows us to obtain a good approach for the electronic spectrum and wave functions, especially for the few lowest energy levels that we will use to calculate the phonon emission rates.

In the quantum dot phonon problem, the eigenmodes and their eigenfrequencies have to be found by taking into account the boundary conditions and the symmetry of the problem. Following the dielectric continuum approximation, the electron-optical phonon interaction Hamiltonian in spherical semiconductor quantum dots as derived from Fröhlich interaction is given by⁵

$$H_\nu = \sum_Q \hbar \omega_\nu C_\nu(Q) [\phi_\nu(Q) a_{\nu Q} + \text{H.c.}], \quad (6)$$

where H.c. stands for Hermitian conjugate. The index Q represents all necessary quantum numbers to specify a phonon state including phonon wave vector and discrete mode indices, $\nu = C$ and S to denote the confined and the surface-type LO phonon, respectively. Also, a_ν is the annihilation operator for phonons in the mode Q , and C_ν are the electron-phonon coupling coefficients. The phonon electrostatic potentials can be written as $\phi_C = j_l(qR) Y_l^m(\Omega)$ for confined modes and $\phi_S = (r/R)^l Y_l^m(\Omega)$ for surface modes, where the values for q are obtained from the boundary condition $j_l(qR) = 0$ at the quantum dot radius R .

Notice that the dielectric continuum approach, used in this work, does not include phonon dispersions as other complex treatments,⁶ where several size-dependent frequencies can coexist. Therefore all LO-confined optical modes are degenerated and display a single bulk LO frequency ω_{LO} , whereas the frequencies of the surface modes will depend only on the quantum number l , as

$$\omega_S^2 = \left[\frac{\epsilon_0 l + \epsilon_D(l+1)}{\epsilon_\infty l + \epsilon_D(l+1)} \right] \omega_{TO}^2, \quad (7)$$

where ϵ_D is the frequency-independent dielectric constant of the surrounding medium, ϵ_0 and ϵ_∞ are the static and the high-frequency dielectric constants, respectively. For spherical dots, these phonon frequencies are independent of number m and their values satisfy the relation $\omega_{TO} < \omega_S < \omega_{LO}$.

We calculate the rate W for an electron scattered from an initial state k to a final state k' , accompanied by the emission of an optical phonon in the mode Q with frequency ω_ν . By using the Fermi's golden rule we can write

$$W_{k \rightarrow k'} = \frac{2\pi}{\hbar} |\mathcal{M}_{k \rightarrow k'}(Q)|^2 \delta(E_k - E_{k'} - \hbar \omega_\nu), \quad (8)$$

where $\mathcal{M}(Q)$ are the matrix elements of the allowed transitions. We use the approach proposed by Vurgaftman and Singh¹⁴ which allows us to include the spectral broadening of the electronic spectra due to a finite energy-level lifetime τ . In order to evaluate the expression (8), we replace the delta function by a Lorentzian line-shape function^{1,2}

$$\delta(E_k - E_{k'} - \hbar \omega_\nu) \rightarrow \frac{1}{\pi} \left[\frac{\Gamma/2}{(E_k - E_{k'} - \hbar \omega_\nu)^2 + (\Gamma/2)^2} \right], \quad (9)$$

where $\Gamma = \hbar/\tau$ is the linewidth and τ is taken to be the reciprocal of the scattering rate W . The set of coupled equations for the scattering rate and for the linewidth are solved numerically, in an iterative procedure, until a chosen convergence condition is achieved.

For our calculations of scattering rates we assume a CdSe spherical quantum dot with radius R embedded in a glass matrix, and use an infinite potential barrier. The material parameters used in our calculations are: the effective mass $m^* = 0.13m_0$, the dielectric constants $\epsilon_0 = 9.56$, $\epsilon_\infty = 6.23$ and $\epsilon_D = 2.25$, the bulk phonon energy $\hbar \omega_{LO} = 26.0$ meV. The calculations are performed at $T \sim 0$ K. The temperature dependence of the one-phonon emission rate is determined from $W = W_0(n_B + 1)$, where n_B is the Bose distribution

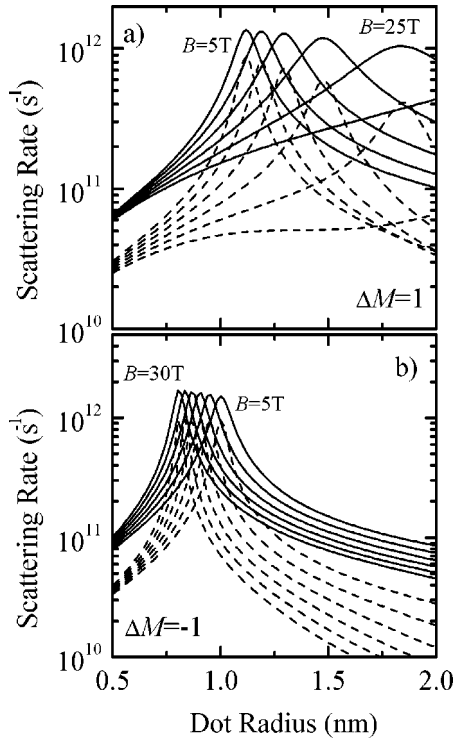


FIG. 1. Scattering rates due to confined and surface modes for transitions: (a) $\Delta M=1$ and (b) $\Delta M=-1$ for a CdSe spherical quantum dot as function of the dot radius.

function and W_0 is the scattering rate for $T=0$ K. In the temperature regime below 50 K, we have $\hbar\omega_p \gg kT$ and Bose function is small, therefore the effect of temperature can be considered as negligible. We will identify the electronic levels by the quantum number M and we restrict our calculations to treat only transitions between the first excited state $M=0, \pm 1$ and the ground state $M=0$. To discuss higher level relaxation, it is necessary to consider multiphonon processes. These processes can involve one-phonon emission of several LO and LA modes, as well as two-phonon emissions (LO \pm LA).²⁰ These processes are not included in this work and are specially important for the high-temperature regime and for larger dot sizes. For simplicity, we have chosen to label the transition $+1 \rightarrow 0$ ($-1 \rightarrow 0$) as $\Delta M=1$ ($\Delta M=-1$).

The calculated electronic relaxation rates due to confined (solid lines) and surface (dashed lines) modes as a function of the dot radius for transitions $\Delta M=1$ and $\Delta M=-1$ are shown in the Figs. 1(a) and (b), respectively. The effects of a magnetic field on transitions between states with $\Delta M=0$ are negligible and will not be shown here. The calculated scattering rates can include contributions of the optic modes with $l>1$, and this establishes an important difference with the free magnetic-field problem where only the mode $l=1$ can contribute to the scattering processes.² It is important to emphasize that the selection rules for transitions involving one-phonon emission in spherical quantum dots are given by the total angular momentum conservation. The change in the symmetry of the wave functions, as induced by the magnetic field, will include the transitions with $l \neq 1$.

As expected, we observe efficient scattering for dot radii such that the separation between the levels involved matches the energy of the emitted phonon ($\Delta E - \hbar\omega_p = 0$, resonant condition). The transition rates progressively broaden and decrease when the energy moves away from the resonance. To interpret our results it is necessary to analyze the dependence of the transition energy with the magnetic field. Within the range of considered magnetic fields, the energy of the transition $\Delta M=1$ ($\Delta M=-1$) is almost linear and with positive (negative) slope as the value of B increases. This implies that the resonance peak for the transition $\Delta M=1$ moves toward a larger dot radius as the intensity of the magnetic field increases, and this effect is illustrated in Fig. 1(a). The opposite effect can be observed in Fig. 1(b) for the transition $\Delta M=-1$. The magnetic-field induced shifts of the resonance peak allow us to select the most efficient phonon-scattering process in a wide range of dot sizes. The effects of the diamagnetic term, proportional to B^2 in the Hamiltonian (1), are important for high magnetic fields ($B > 15$ T). Another important characteristic of our results is the additional broadening in the scattering rate peaks induced by the magnetic field. This broadening is particularly important for the transitions $\Delta M=1$. This behavior can be explained by noticing that the transition probability per unit time in a two-level system is, in general, proportional to $|\mathcal{M}|^2 / \sqrt{|\mathcal{M}|^2 + [\Delta E(B)]^2}$, where $\Delta E(B)$ represents the transition energy with emission of a phonon $\hbar\omega_p$, in presence of a magnetic field B . Therefore any change in the intensity produced by the magnetic field will also cause variations in the broadening of the peak transition rate. It is clear that the increase or decrease of the peak broadening will depend strongly on the sign of the term $\Delta M \hbar\omega_C$. Additionally, we observe for transitions $\Delta M=1$, the intensity of the scattering decreases as the magnetic field increases. The opposite behavior is observed for transitions $\Delta M=-1$. The transition probability is proportional to the electron-phonon overlap integral, thus a close look on the variation in the shape of the wave function with the field becomes necessary in order to explain the behavior of the peak intensity close to the resonance. It is clear that the combination of magnetic and spatial confinements will determine the value of the overlap. In general, when the spatial confinement is strong, the magnetic field produces an additional spatial confinement of the electronic wave functions. Thus the confined phonon modes will have larger overlap integrals. In situations of weak spatial confinement, the magnetic field shrinks the carrier wave function producing the decrease of the overlap integral. An increment in the overlap of up to 5% can be observed for quantum dots with radius $R < 100$ Å and a decrease of approximately 10% in dots larger than 100 Å. The magnetic-field effects on the electron-phonon overlap are similar for surface modes.

On the other hand, the rates for surface phonons are smaller than for confined modes as a direct consequence of the behavior of radial overlap integrals. The surface phonon potentials are strongly localized at the interface region, therefore they couple weakly with the carrier wave functions which are mainly localized inside the dot.

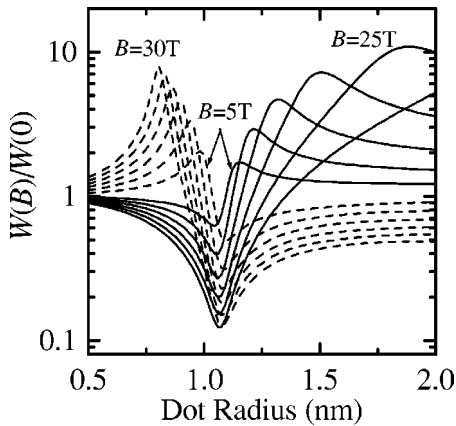


FIG. 2. Ratio of the scattering rates in a magnetic field $W(B)$ and free magnetic-field rates $W(0)$ as function of the dot radius. Confined and surface modes contributions are included. Solid (dashed) lines are for $\Delta M=1$ ($\Delta M=-1$) transition.

For larger radii ($R > 300 \text{ \AA}$), the total scattering rate (confined + interface) for zero magnetic field converges to the CdSe bulk scattering rates W_b . The rates for $B=0$ presented in our previous work² show more clearly this convergence. Following Ridley,²¹ we have estimated the bulk CdSe scattering rate $W_b = 3.5 \times 10^{12} \text{ s}^{-1}$.

Furthermore, we will compare the calculated scattering rates with the free magnetic-field rates, and this gives a direct measure of the effects of the magnetic confinement and the B dependence of the transition energy on the scattering rates. For high magnetic fields, these effects can be better illustrated in Fig. 2 where we display the ratio $W(B)/W(0)$, where $W(B)$ is the total scattering rate in presence of magnetic field B and $W(0)$ is the total scattering rate in absence of field. For the transitions considered in this work, strong fields produce more remarkable changes on the scattering rates. For instance, at 25 T the $\Delta M=1$ transition of the

magnetic scattering rate can be up to ten times larger than the free magnetic-field rate.

Finally, the inclusion of the acoustic modes in the calculation is an important aspect that should be considered in a future work. It has been shown that at $B=0$, the contributions of acoustic modes to the scattering rates are significant.^{1,20} In our previous work,¹ we have studied the dependence of ripple mechanism (RM) and deformation potential (DP) with the quantum dot size as well as their contributions to the electron–acoustic-phonon scattering rate. As discussed above, an external magnetic field modifies the electron–phonon overlap integral. By noting the nature of the RM coupling (dominant for small size dots), we expected stronger changes in the rates in the presence of the magnetic field. The rates due to DP (important for large dot sizes) would not be modified significantly by the field. Additionally, the dependence of the transition energy with B opens alternatives to adjusting size ranges where the RM or DP are dominant. Obviously, the effects of the glass matrix on the acoustic-mode frequencies should be taken into account.

In conclusion, we have discussed the effects of the magnetic field on the interaction of the electrons with confined and surface optical phonons in CdSe spherical quantum dots. Our calculations show that the scattering rates are sensitive to the applied magnetic field and that alternative scattering channels can become efficient by magnetic tuning in a wide range of dot radius. Using a simple expression that relates the scattering rates with the transition energy, we have explained the additional peak broadening induced by the magnetic field. Finally, we discussed how the magnetic field modifies the carrier wave functions and produces an enhancement in the scattering rates. This effect is particularly important at high magnetic fields.

This work has been supported by Fundação de Amparo à Pesquisa do Estado de São Paulo (FAPESP) and Conselho Nacional de Desenvolvimento Científico e Tecnológico (CNPq).

¹A. M. Alcalde, G. E. Marques, G. Weber, and T. L. Reinecke, *Solid State Commun.* **116**, 247 (2000).
²A. M. Alcalde and G. Weber, *Semicond. Sci. Technol.* **15**, 1082 (2000).
³M. Betz *et al.*, *Phys. Rev. Lett.* **86**, 4684 (2001).
⁴J. Urayama, T. B. Norris, J. Singh, and P. Bhattacharya, *Phys. Rev. Lett.* **86**, 4930 (2001).
⁵M. C. Klein, F. Hache, D. Ricard, and C. Flytzanis, *Phys. Rev. B* **42**, 11 123 (1990).
⁶E. Roca, C. Trallero-Giner, and M. Cardona, *Phys. Rev. B* **49**, 13 704 (1994).
⁷R. Rinaldi *et al.*, *Phys. Rev. B* **53**, 13 710 (1996).
⁸W. Heller and U. Bockelmann, *Phys. Rev. B* **55**, R4871 (1997).
⁹N. Miura, Y. H. Matsuda, K. Uchida, and H. Arimoto, *J. Phys.: Condens. Matter* **11**, 5917 (1999).
¹⁰M. Bayer, A. Schmidt, A. Forchel, and F. Faller, *Phys. Rev. Lett.*

74, 3439 (1999).

¹¹R. Haupt and L. Wendler, *Solid-State Electron.* **37**, 1153 (1994).
¹²S. Nomura *et al.*, *J. Lumin.* **70**, 144 (1996).
¹³Z. Xiao, *J. Appl. Phys.* **86**, 4509 (1999).
¹⁴I. Vurgaftman and J. Singh, *Appl. Phys. Lett.* **64**, 232 (1994).
¹⁵H. X. Jiang, *Phys. Rev. B* **35**, 9287 (1987).
¹⁶Z. Xiao, J. Zhu, and F. He, *J. Appl. Phys.* **79**, 9181 (1996).
¹⁷L. Bányai and S. W. Koch, *Semiconductor Quantum Dots, Series on Atomic, Molecular and Optical Physics* (World Scientific Publishing Co. Pte. Ltd., Singapore, 1993).
¹⁸D.-S. Kim *et al.*, *Phys. Rev. Lett.* **68**, 1002 (1992).
¹⁹P. A. Knipp and T. L. Reinecke, *Phys. Rev. B* **54**, 1880 (1996).
²⁰T. Inoshita and H. Sakaki, *Phys. Rev. B* **46**, 7260 (1992).
²¹B. K. Ridley, *Quantum Processes in Semiconductors*, 3rd. (Oxford Science Publications, Oxford, 1993).